Cancer Immunology, Immunotherapy
https://doi.org/10.1007/s00262-021-02874-y

ORIGINAL ARTICLE

The cytokine milieu compromises functional capacity of tumor-infiltrating plasmacytoid dendritic cells in HPV-negative but not in HPV-positive HNSCC

Vladimír Koucký[1,2] · Kamila Hladíková[1] · Eliška Táborská[1] · Jan Bouček[2] · Marek Grega[3] · Radek Špíšek[1] · Anna Fialová[1]

Received: 20 July 2020 / Accepted: 25 January 2021

Abstract

Plasmacytoid dendritic cells (pDCs) are the most potent type I interferon-producing cells and play an important role in antiviral immunity. Tumor-infiltrating pDCs were shown to be predominantly pro-tumorigenic, with reduced ability to produce interferon alpha (IFNα) and confirmed capacity to prime regulatory T cells (Tregs) by the ICOS/ICOS-L pathway. Because a significant number of HNSCCs are induced by human papillomaviruses and show markedly different immune profiles than non-virally induced tumors, we compared the phenotype and functional capacity of HNSCC-infiltrating pDCs to the HPV status of the tumor. We observed a reduced capacity of pDCs to produce IFNα upon toll-like receptor activation in HPV-negative samples and a rather uncompromised functionality in HPV-associated tumors. Additionally, supernatants from non-virally induced but not HPV-associated tumor cell suspensions significantly inhibited IFNα production by peripheral blood-derived pDCs. We identified IL-10 and TNFα as the soluble pDC-suppressive factors with the highest variability between HPV-negative and HPV-positive tumor-derived supernatants. Additionally, we observed a positive correlation of tumor-infiltrating pDCs with Tregs in HPV-negative samples but not in virally induced tumors. Overall, our study indicates that the immunosuppressive cytokine milieu rich in IL-10 and TNFα in HPV-negative but not in HPV-positive HNSCC significantly affects the functional capacity of tumor-infiltrating pDCs, and such dysfunctional pDCs may further support the immunosuppressive tumor microenvironment by promoting the expansion of Tregs in the tumor tissue.

Keywords Head and neck cancer · Human papillomavirus · Plasmacytoid dendritic cells · Interferon alpha

Introduction

The typical risk factors for the development of head and neck squamous cell carcinoma (HNSCC) are smoking and alcohol consumption. However, in the last two decades, infection with high-risk strains of human papillomavirus (HPV) has been identified as a significant etiologic agent of HNSCC carcinogenesis [1, 2]. HPV-induced tumors are typically located in the oropharynx and are associated with longer overall survival in response to conventional treatment [3, 4]. The established indicator of HPV status in oropharyngeal squamous cell carcinoma (OPSCC) is the overexpression of p16INK4a (p16) protein [5, 6]. Current guidelines of the American Joint Committee on Cancer and The National Comprehensive Cancer Network regard $p16^+$ OPSCC as a specific HNSCC subtype with its own staging system [6, 7]. There are ongoing studies focused on the treatment de-escalation of HPV^+ OPSCCs that could decrease the toxic side effects of the established therapeutic regimens [8]. Moreover, new immunotherapeutic approaches, namely checkpoint blockers nivolumab [9] and pembrolizumab [10], are changing the standard therapeutic protocols for HNSCC. Despite significant advances in therapy, HNSCC is still characterized

✉ Vladimír Koucký
koucky@sotio.com

✉ Anna Fialová
fialova@sotio.com

1 Sotio, Prague, Czech Republic

2 Department of Otorhinolaryngology and Head and Neck Surgery, First Medical Faculty, Motol University Hospital, Prague, Czech Republic

3 Department of Pathology and Molecular Medicine, Second Medical Faculty, Motol University Hospital, Prague, Czech Republic

Published online: 11 February 2021

by high morbidity, emphasizing the need for further research on the tumor microenvironment.

The profile of the immune cells infiltrating the tumor microenvironment was identified as one of the crucial elements in the course of the disease. Differences in the cytokine production and immune infiltrate pattern of HPV^+ and HPV^- HNSCC were described by several authors, reporting higher immune cell infiltration and less-pronounced immunosuppressive setting in HPV^+ tumors [11–13]. However, differences in the phenotype and function of plasmacytoid dendritic cells (pDCs), the key players in antiviral immunity, have not been evaluated with respect to the HPV status in HNSCC so far. Human pDCs are characterized by substantial production of IFNα and the expression of specific markers BDCA-2 and BDCA-4 [14, 15]. Additionally, a wide variety of functions have been assigned to pDCs, such as antigen presentation [16], regulatory T cell (Treg) induction [17], cell-to-cell cytotoxicity [18] and attraction and activation of innate immune cells [19].

In tumor immunology, the impact of pDCs was reported to be rather pro-tumorigenic [20]. Tumor-infiltrating pDCs were shown to be functionally impaired, and high levels of pDCs positively correlated with poor prognosis in breast, ovarian and skin cancer [21–23]. In agreement with these studies, pDCs infiltrating HNSCC were found to be functionally impaired [24] and had a negative prognostic impact [25, 26]; however, a correlation with the HPV status was not discussed.

In this study, we performed a phenotypic and functional analysis of the tumor-infiltrating pDCs in HNSCC and focused on the differences between HPV^- and HPV^+ tumors. For the first time, we show that pDCs infiltrating HPV^+ HNSCC have a significantly higher capacity to produce IFNα compared to pDCs infiltrating HPV^- tumors, most likely due to a markedly different cytokine milieu in the tumor microenvironment.

Materials and methods

Patients and samples

Freshly resected primary HNSCC specimens were obtained from 76 patients who underwent therapeutic surgery at the Motol University Hospital in Prague, Czech Republic, between October 2016 and May 2019. Control peritumoral mucosa was obtained from 9 patients. Control tonsils were obtained from 9 healthy age-matched donors undergoing surgery for a sleep apnea syndrome. None of the cancer patients enrolled in this study had received any neoadjuvant treatment. All of the patients signed an informed consent form approved by the Ethics Committee of the Motol University Hospital. Pathologic staging of HNSCC specimens was performed according to the 8th edition of the American Join Committee on Cancer. The clinical and pathological characteristics of the patients are summarized in Table 1.

Fresh tumor and control tissue samples processing

Fresh tissues were minced with scissors and digested in RPMI 1640 (Thermo Fisher Scientific) containing 1 mg/ml of collagenase D (Roche) and 0.05 mg/ml DNase I (Roche) for 30 min at 37 °C under a gentle rocking motion. Subsequently, the specimens were passed through a 100-µm nylon cell strainer (BD Biosciences) and washed with PBS (Lonza).

Table 1 Clinical and pathological characteristics of the patients

Variable	Patients	
	No.	%
Total no. of patients	76	
Age		
Mean	61	
Range	38—80	
Sex		
Male	61	80.3
Female	15	19.7
Tumor site		
Palatine tonsil	19	25
Base of the tongue	12	15.8
Oropharynx NS	6	7.9
Body/margin of the tongue	7	9.2
Base of the mouth	5	6.6
Hypopharynx	5	6.6
Larynx	22	28.9
T status		
T1	7	9.2
T2	38	50
T3	16	21.1
T4	15	19.7
N status		
N0	26	34.2
N1	28	36.8
N2	22	29
N3	0	0
Stage		
I	22	29
II	12	15.8
III	15	19.7
IV	27	35.5
HPV status		
HPV +	32	42.1
HPV –	44	57.9

Flow cytometry

Single-cell suspensions derived from tumor and control tissues were labeled using a panel of monoclonal antibodies listed in Supplementary Table 1. In some of the patients ($n = 33$), cell suspensions were incubated with CpG ODN 2216 (20 ug/ml) or imiquimod (5 ug/ml, InvivoGen) in the presence of brefeldin A for 5 h. For intracellular detection of cytokines and FoxP3, cells were fixed and permeabilized with a Fixation/Permeabilization Buffer Set (eBioscience) and intracellularly labeled with primary antibodies. Cells were analyzed on a BD LSRFortessa (BD Biosciences) and evaluated with FlowJo software (TreeStar).

Detection of soluble factors in cell culture supernatants

Tumor-derived single-cell suspensions (1×10^6 cells/ml) were cultured in 96-well U-bottom plates with CpG oligonucleotides (CpG ODN) 2216 (20 µg/ml) or imiquimod (5 µg/ml) in RPMI 1640 supplemented with 10% heat-inactivated FCS, L-glutamine and penicillin–streptomycin (complete RPMI 1640). After 24 h of incubation, cell culture supernatants were harvested and stored at − 80 °C until use. To detect the concentrations of IFNα, IFNγ, TNFα, IL-3, IL-4, IL-6, IL-10, IL-12α and IL-17, the Luminex-based MILLIPLEX™ Human Cytokine Kit (Merck) was used. HMGB1 was detected using ELISA (IBL International).

RNA extraction from tumor cell suspensions and quantitative real-time PCR

Total RNA was isolated from 1×10^6 HNSCC-derived cells using the RNA Easy Mini Kit (Qiagen). The concentration and purity of the samples were determined by spectrophotometry with a NanoDrop© 2000c (Thermo Fisher Scientific), and the RNA integrity was assessed using a 2100 Bioanalyzer (Agilent). Complementary DNA was synthesized from 100 ng of total RNA using the iScript cDNA Synthesis Kit (Bio-Rad). The gene expression levels of IL-10, TNFα, TGFβ and the β-actin housekeeping gene were evaluated using the CFX 96™ Real-Time System (Bio-Rad). The specificity of the amplified PCR product was assessed using an Agilent DNA 1000 Kit (Agilent). The relative expression of the target genes was normalized to the expression of β-actin.

Isolation and activation of pDCs in the presence of HNSCC culture supernatants

Peripheral blood mononuclear cells (PBMCs) were isolated from the peripheral blood of healthy donors using Ficoll-Paque density gradient solution (GE Healthcare). Plasmacytoid DCs were isolated from PBMCs using a BDCA-4 magnetic separation kit (Miltenyi Biotec). A 100 × enriched pDCs were seeded in a 96-well U-bottom plate at a concentration of 2.5×10^5/ml and incubated with HPV^+ and HPV^- HNSCC-derived culture supernatants upon stimulation with 5 µg/ml CpG ODN 2216. Alternatively, pDCs were cultured in complete RPMI 1640 with the addition of recombinant cytokines (IL-6, IL-10, TNFα at 5–10 ng/ml, PeproTech) upon stimulation with 5 µg/ml CpG ODN 2216. In part of the experiments, neutralizing antibodies against IL-6, IL-10 and TNFα (BioLegend) were added to the cultures at a concentration of 10 µg/ml. After 24 h of incubation, supernatants were collected, and levels of IFNα were measured using an IFNα ELISA kit (PBL Assay Science). The reference value of IFNα (100% production) was assessed as the level of IFNα produced upon CpG stimulation in complete RPMI 1640. The level of inhibition was expressed as a proportional change of IFNα production with respect to the reference value of each donor.

Treg generation

Purified pDCs prepared as described above were seeded in a 96-well U-bottom plate at a concentration of 5×10^5 pDCs/well and incubated with/without HPV^+ or HPV^- HNSCC-derived culture supernatants overnight. After washing in PBS, purified autologous $CD4^+$ T cells were added in a ratio of 1:5. After 5 days of incubation, the proportion of $CD4^+CD25^{hi}FoxP3^+$ Tregs was analyzed using flow cytometry. As multiple donors were used, the frequency of Tregs was normalized to control. The reference value (100%) was assessed based on the proportion of Tregs in co-cultures of $CD4^+$ T cells with control pDCs cultivated in complete RPMI.

Immunohistochemistry (IHC)

Staining was carried out on FFPE sections following deparaffinization and antigen retrieval. Endogenous peroxidase activity was blocked with 3% hydrogen peroxide. Sections were incubated with protein block reagent (DAKO) and stained with primary antibodies against BDCA-2 (goat IgG, R&D Systems), FoxP3 (mouse IgG1, Abcam), IL-6 (rabbit IgG, Abcam), IL-10 (mouse IgG1, Abcam) and TNFα (mouse IgG1, Abcam) followed by determination of enzymatic activity. Sections were counterstained with hematoxylin or nuclear fast red (Vector Laboratories).

HPV detection

IHC

The antibody p16INK4a (monoclonal mouse anti-human p16, Clone G175-405, BD Pharmingen, dilution 1:100) was

used. The intensity of the staining (graded + to + + +) and the proportion of stained cells (scored as percentages) were evaluated. For p16 immunostaining, the location of the signal (cytoplasmic and/or nuclear) was also specified. A semi-quantitative evaluation was performed. Samples positive for p16 expression had to show more than 70% of positive cells and reveal nuclear and/or cytoplasmic staining.

PCR

HPV DNA from the paraffin-embedded tissue was extracted with the MagCore Genomic DNA FFPE One-Step Kit (RBC Bioscience). HPV DNA detection and genotyping were performed by qualitative real-time PCR with the AmoyDx Human Papillomavirus Genotyping Detection Kit (Amoy Diagnostics). HPV DNA + /p16 + samples were considered HPV-positive.

Statistical analysis

Statistical analyses were performed using Statistica® 10.0 software (StatSoft). The parametric assumptions of the data were verified using the Kolmogorov–Smirnov test for normality. The homogeneity of the variances was tested by the Levene test. The differences between HPV-positive and HPV-negative tumor samples were analyzed using the Mann–Whitney U test. The differences between the reference value and the experimental value were analyzed using a t test. The correlation between the levels of pDCs and the levels of Tregs was evaluated using Pearson's chi-square test. The results were considered statistically significant when $p < 0.05$.

Results

The proportions of pDCs infiltrating HPV$^+$ tumors are comparable to those of HPV$^-$ HNSCC samples and healthy peritumoral mucosa

To evaluate the density of tumor-infiltrating pDCs in relation to HPV status, we analyzed cell suspensions from 32 HPV$^+$ and 44 HPV$^-$ HNSCC samples using flow cytometry. All of the HPV$^+$ tumors were localized in the oropharynx. HPV$^-$ tumors were localized in the larynx, the hypopharynx, base of the mouth, body/margin of the tongue and the oropharynx, as indicated in Table 1. The pDCs were defined as CD45$^+$Lin$^-$CD4$^+$CD123$^+$BDCA2$^+$ (Fig. 1a). Healthy tonsils and peritumoral mucosa of HNSCC patients were used as control tissues. The proportions of tumor-infiltrating pDCs did not differ between HPV$^+$ and HPV$^-$ tumors ($0.13 \pm 0.23\%$ and $0.11 \pm 0.14\%$ of total cells, respectively; Fig. 1b). The results were similar when the proportions of CD45$^+$ cells ($0.19 \pm 0.26\%$ and $0.24 \pm 0.26\%$, respectively; Fig. 1c) were compared. No correlations of pDC proportions with the clinical and pathological characteristics of HNSCC patients were found.

Plasmacytoid DCs from HPV$^-$ HNSCC samples show impaired responsiveness to TLR7 and TLR9 stimulation, whereas pDCs infiltrating HPV$^+$ tumors remained functionally unimpaired

To estimate the functionality of HNSCC-infiltrating pDCs, we stimulated tumor-derived and control tonsil-derived cell suspensions with imiquimod (IMQ), a TLR7 agonist,

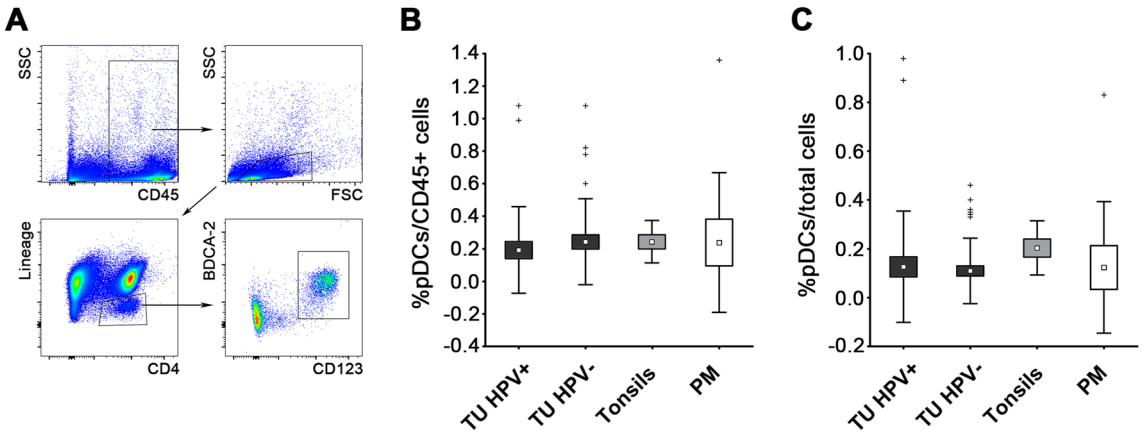

Fig. 1 Flow cytometric analysis of pDC frequency in freshly resected tissues of HPV$^+$ HNSCC samples ($n = 32$), HPV$^-$ HNSCC samples ($n = 44$), age-matched tonsils from healthy donors ($n = 9$) and macroscopically tumor-free peritumoral mucosa (PM, $n = 9$). Box plots represent proportions of pDCs when gated on total cells **a** and CD45$^+$ cells **b**. Boundaries of the box indicate the standard error of the mean (SEM), and the squares in the box represent the mean. Whiskers indicate the standard deviation (SD), crosses represent outliers. **c** Dot plots show the gating strategy in a representative HPV$^+$ tumor sample

and CpG ODN 2216 (CpG), a TLR9 agonist, and analyzed IFNα production by pDCs. Plasmacytoid DCs from HPV$^+$ tumors produced significantly higher amounts of IFNα upon CpG stimulation based on the mean fluorescence intensity (MFI) (4137 ± 3346 vs. 7879 ± 4272 for HPV$^-$ and HPV$^+$ samples, respectively; Fig. 2b), although there were no differences in the proportions of IFNα-producing cells (3.2 ± 5.4 vs. 3.0 ± 3.1; Fig. 2a). This result was supported by the significantly higher levels of IFNα in HPV$^+$ tumor-derived cell culture supernatants after CpG stimulation (240.7 ± 380.8 pg/ml for HPV$^-$ cultures vs. 971.8 ± 1461 pg/ml for HPV$^+$ cultures; Fig. 2c). The levels of IFNα produced by HPV$^+$ tumor-derived pDCs were comparable to the levels produced by pDCs from control tonsillar tissue (893 ± 1431 pg/ml; Fig. 2c). The trend was similar upon imiquimod stimulation; however, the differences also did not reach statistical significance. Additionally, we observed markedly lower levels of IFNα production in HPV$^+$ cell suspensions obtained from patients who eventually succumbed to the disease compared to patients in remission (Fig. 2d). Upon TLR stimulation, 71 ± 5.2% of IFNα$^+$ cells co-expressed pDC-associated markers CD123 and BDCA2. (Representative staining is shown in Fig. S1A.)

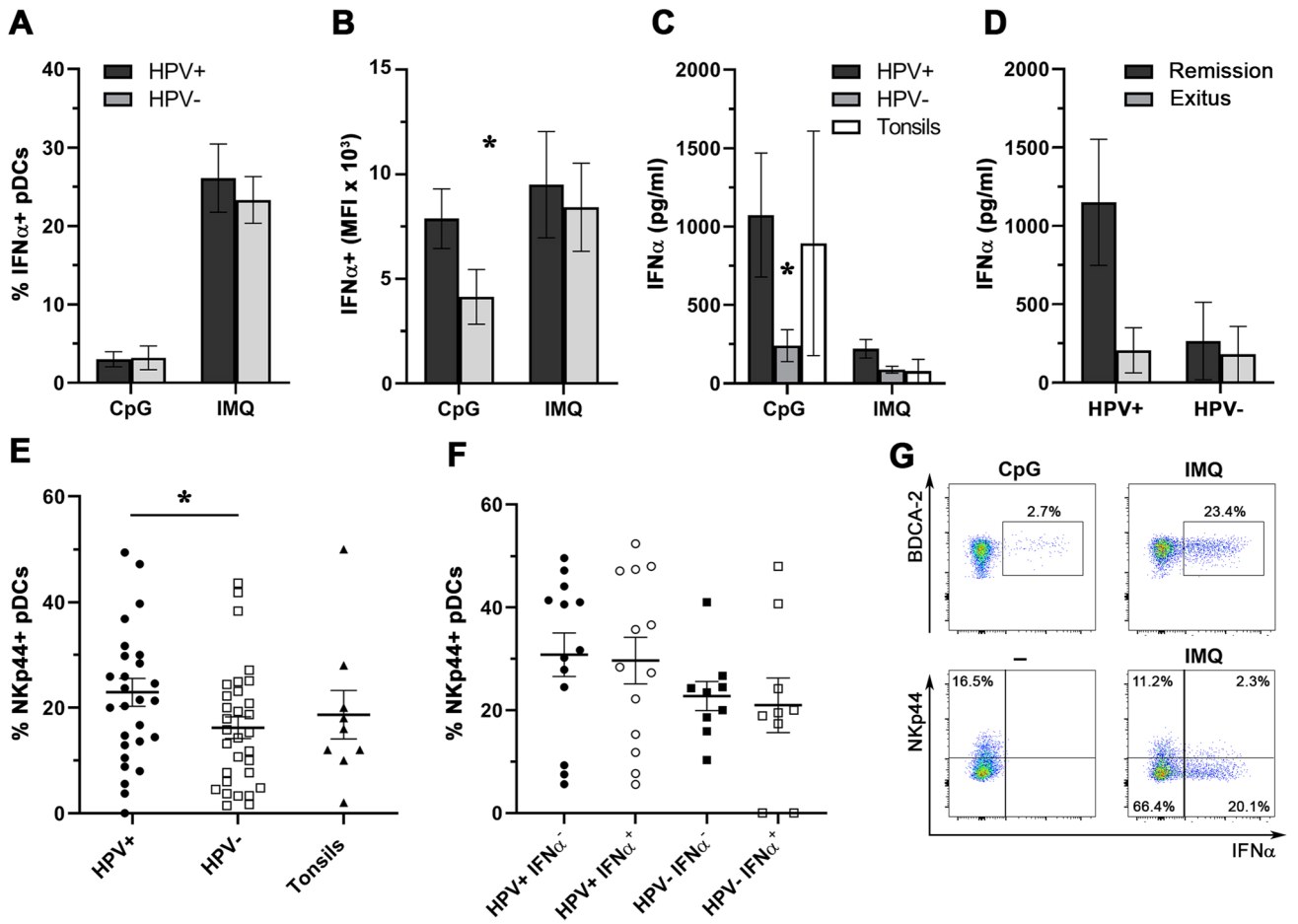

Fig. 2 Differences in IFNα production and NKp44 expression in pDCs infiltrating HPV$^+$ and HPV$^-$ HNSCC samples. Columns represent **a** the mean proportions of tumor-infiltrating IFNα-producing pDCs upon stimulation with CpG ODN 2216 (CpG; 20 μg/ml, 5 h) or imiquimod (IMQ; 5 μg/ml, 5 h); **b** the mean fluorescence intensity (MFI) of IFNα$^+$ pDCs upon stimulation with CpG or IMQ; and **c** the mean concentration of IFNα in tissue-derived cell culture supernatants derived from HPV-positive HNSCC ($n=16$), HPV-negative HNSCC ($n=14$) and control tonsils ($n=4$) after 24 h of stimulation with CpG or IMQ. All error bars indicate SEM. **d** Columns show differences in CpG-induced IFNα production in cell culture supernatants obtained from HPV$^+$ and HPV$^-$ tumor samples with respect to patient overall survival. **e** Dot plot showing proportions of NKp44$^+$ pDCs derived from HPV$^+$ HNSCC ($n=28$), HPV$^-$ HNSCC ($n=31$) and age-matched control tonsils ($n=9$). Each symbol represents a patient, the horizontal line represents the average, and error bars indicate SEM. **f** Dot plot showing proportions of IMQ-stimulated IFNα$^+$ pDCs derived from HPV$^+$ HNSCC ($n=13$) and HPV$^-$ HNSCC ($n=9$) in relation to NKp44 expression. The horizontal line represents the average, and error bars indicate SEM. **g** Dot plots showing the production of IFNα and expression of NKp44 in a representative patient. *$p<0.05$

Plasmacytoid DCs derived from HPV$^+$ HNSCC showed higher expression of NKp44 compared to those from HPV$^-$ samples

To characterize the phenotype of HNSCC-infiltrating pDCs in detail, we assessed the expression levels of TLR7, TLR9, CD28, NKp44, Granzyme B, IDO, TIM-3 and TRAIL. With the exception of NKp44, there were no statistically significant differences between HPV$^+$ and HPV$^-$ tumor-infiltrating pDCs in the expression of the evaluated molecules. Surprisingly, the proportion of NKp44-expressing pDCs was significantly higher in HPV$^+$ tumors compared to HPV$^-$ samples (22.9 ± 14% vs. 16.2 ± 11.4%, respectively; Fig. 2e). Although NKp44 has been described as an inhibitory molecule in pDCs upon artificial activation, the proportion of IFNα-producing cells was similar in NKp44$^+$ and NKp44$^-$ BDCA-2$^+$CD123$^+$ cells (26.9% and 25.1%, respectively). The proportions were similar when the samples were grouped by HPV$^+$ and HPV$^-$ status (Fig. 2f).

Supernatants derived from HPV$^-$ but not HPV$^+$ HNSCC inhibit IFNα production by control pDCs

We tested the effect of HPV$^+$ (n = 12) and HPV$^-$ (n = 12) HNSCC-derived cell culture supernatants on pDCs isolated from PBMCs of healthy donors (n = 4). The production of IFNα was markedly inhibited in the presence of culture supernatants harvested from HPV$^-$ tumor-derived cell suspensions but not in the presence of cell culture supernatants obtained from HPV$^+$ tumors (Fig. 3a).

To reveal the possible soluble factors responsible for IFNα inhibition induced by HPV$^-$ tumor samples, we analyzed the production of IFNγ, TNFα, IL-3, IL-4, IL-6, IL-10, IL-12, IL-17A and HMGB1 in culture supernatants of both HPV$^-$ and HPV$^+$ tumor-derived cell suspensions. In comparison with HPV$^+$ tumor samples, HPV$^-$ tumor-derived cell suspensions produced significantly higher levels of IL-6, IL-10 and TNFα (Fig. 3b). Additionally, we evaluated the mRNA expression of the three major IFNα inhibitors reported in the literature, namely IL-10, TNFα and TGFβ. The relative mRNA expression of TNFα was significantly higher in HPV$^-$ tumor-derived cell suspensions. Surprisingly, there was no difference in the expression levels of TGFβ mRNA between HPV$^-$ and HPV$^+$ tumor samples (Fig. 3c).

TNFα in the microenvironment of HPV$^-$ tumors seems to be the major inhibitor of IFNα production by pDCs

To further investigate the impact of IL-6, IL-10 and TNFα on IFNα production, the recombinant cytokines were added to cultures at concentrations corresponding to the levels observed in HPV$^-$ tumor-derived cell culture supernatants (5–10 ng/ml). Of all of the factors tested, IL-10 and TNFα significantly inhibited the production of IFNα by control pDCs (Fig. 3d). To directly confirm the role of tumor-derived IL-10 and TNFα in pDC inhibition, we incubated control pDCs with HPV$^-$ tumor-derived cell culture supernatants in the presence of IL-6, IL-10 and TNFα neutralizing antibodies. For assessment of expected values, pDCs were incubated with recombinant IL-6, IL-10 and TNFα and respective neutralizing antibodies (Fig. 3e). The neutralization of TNFα was the most potent and restored the capacity of pDCs to produce IFNα to 101 ± 5.9% in pDC cultures with recombinant cytokines and to 82.8 ± 13.5% in pDC cultures with HPV$^-$ cell culture supernatants, whereas neutralization of IL-10 restored the IFNα production to 44.2 ± 9.4 and 47.3 ± 19.9%, respectively. Neither synergistic, nor additive effect was observed after neutralization of more cytokines simultaneously (Fig. 3e, f).

Tumor cells are an important source of IL-6, IL-10 and TNFα in HPV$^-$ HNSCC samples

To describe the major source of IL-6, IL-10 and TNFα in the tumor microenvironment, we analyzed the expression of these cytokines in HPV$^+$ and HPV$^-$ HNSCC tissue sections. Whereas IL-6, IL-10 and TNFα were detected in the tumor epithelium of 80%, 72.7% and 81.8% of HPV$^-$ samples, respectively, the proportions of HPV$^+$ samples expressing these cytokines in the tumor cells were markedly lower, namely 50%, 14.3% and 50% (Fig. 4a). Representative IHC staining is shown in Fig. 4b.

Treg proportions correlate with pDC proportions in HPV$^-$ HNSCC

In the tumor microenvironment, pDCs have been reported to be capable of inducing/expanding Tregs. Although there was no statistically significant difference in the average level of Treg proportions (defined as CD4$^+$CD127$^{-/lo}$CD25^{hi}FoxP3$^+$) evaluated by flow cytometry (Fig. 5a) or absolute numbers of FoxP3$^+$ lymphocytes in the tumor epithelium and stroma (Fig. 5d) between HPV$^+$ and HPV$^-$ HNSCC, we observed a strong positive correlation of proportions of tumor-infiltrating pDCs and Tregs in HPV$^-$, but not HPV$^+$ tumor samples (Fig. 5b–c). Additionally, we observed clear colocalization of FoxP3$^+$ Tregs and BDCA-2$^+$ pDCs in the tumor stroma, indicating possible interactions between pDCs and Tregs in the tumor microenvironment (Fig. 5e).

Supernatants derived from HPV$^-$ but not HPV$^+$ HNSCC shape pDCs to favor Treg expansion

To assess the capability of pDCs to induce Treg expansion in HPV$^-$ HNSCC microenvironment, we cultivated pDCs

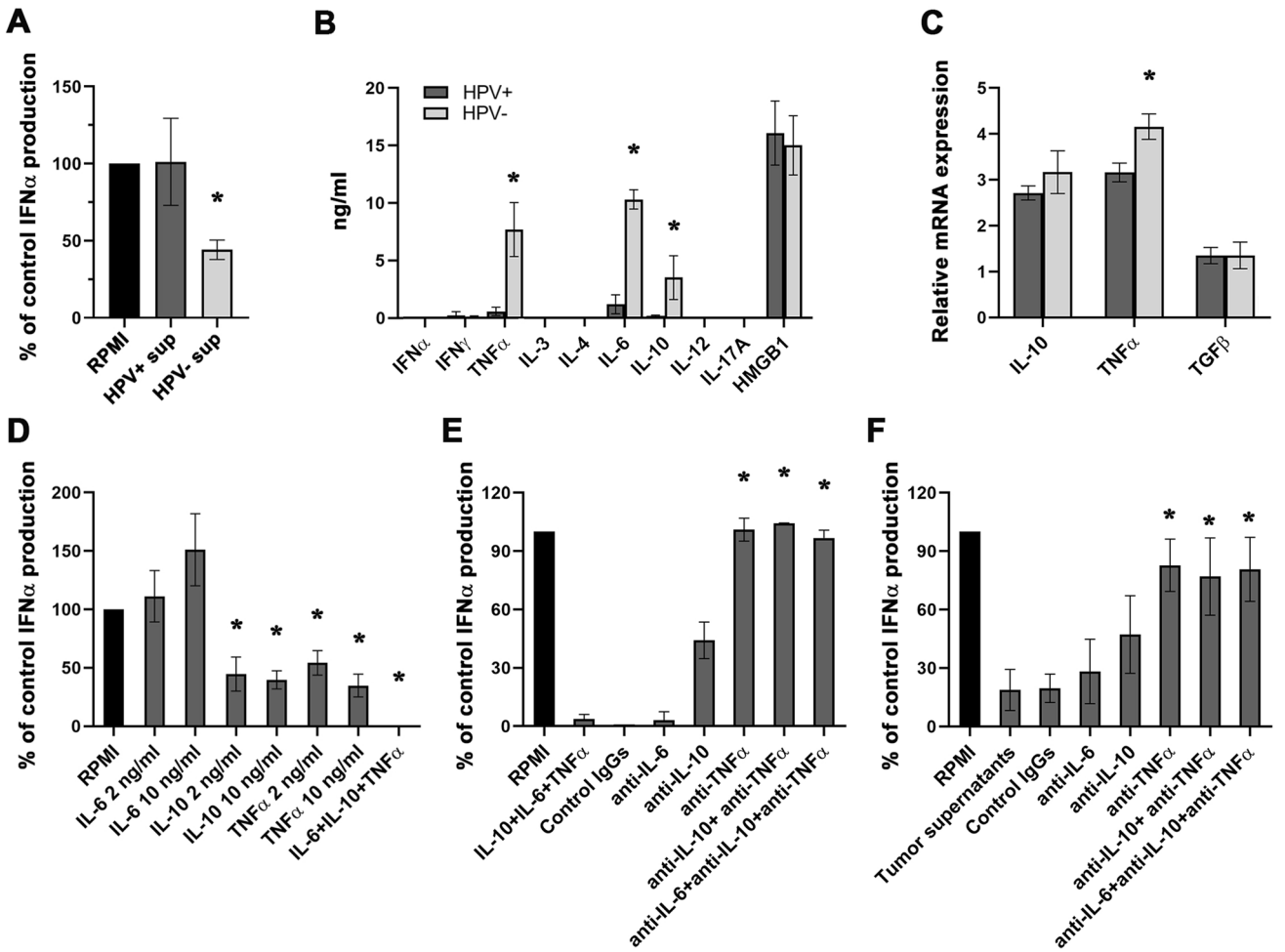

Fig. 3 The effect of HPV$^+$ and HPV$^-$ tumor-derived cell culture supernatants on CpG-induced IFNα production in pDCs. **a** BDCA-2$^+$ pDCs were isolated from the peripheral blood of healthy donors ($n=4$) and incubated in the presence of tumor supernatants ($n=18$) and CpG ODN 2216 (5 µg/ml). The reference value (100%) indicates the production of IFNα upon CpG stimulation in complete RPMI medium and was evaluated for each donor individually. Columns represent the mean proportion of the reference production of IFNα ± SEM. **b** Columns represent differences in levels of selected cytokines in highly suppressive (> 50%) HPV$^-$ cell culture supernatants ($n=5$) and supernatants from non-suppressive HPV$^+$ tumor-derived cell suspensions ($n=5$). **c** Columns show the mean (± SEM) relative IL-10, TNFα and TGFβ mRNA expression in HPV$^+$ ($n=4$) and HPV$^-$ ($n=6$) tumor samples. **d** Effect of the indicated recombinant cytokines on CpG ODN 2216-induced IFNα production in healthy control blood-derived pDCs. The reference value (100%) indicates the IFNα level after the addition of RPMI only. Columns represent the mean proportion of the reference production ± SEM in three separate experiments performed with 8 different donors. **e** Columns represent IFNα production changes in pDC cultures with recombinant IL-6, IL-10 and TNFα in the presence or absence of anti-IL-6, anti-IL-10 and anti-TNFα neutralizing antibodies (10 µg/ml). Antibody-treated samples were compared to samples with recombinant cytokines. **f** Columns represent IFNα production changes in pDC cultures with HPV$^-$ cell culture supernatants in the presence or absence of anti-IL-6, anti-IL-10 and anti-TNFα neutralizing antibodies (10 µg/ml). Antibody-treated samples were compared to samples with culture supernatatnts.*$p < 0.05$

from healthy donors with HPV$^+$ and HPV$^-$ HNSCC cell culture supernatants. Subsequently, supernatant-experienced pDCs were co-cultured with autologous CD4$^+$ T cells. As expected, pDCs affected by HPV$^-$ HNSCC supernatants generated significantly higher numbers of Tregs compared to control pDCs and pDCs influenced by HPV$^+$ HNSCC supernatants (Fig. 5f).

Discussion

Plasmacytoid DCs have been widely reported as dysfunctional and pro-tumorigenic in solid tumors, including HNSCC [20, 24, 27, 28]. However, HNSCC is a heterogeneous group of tumors caused by two major etiological

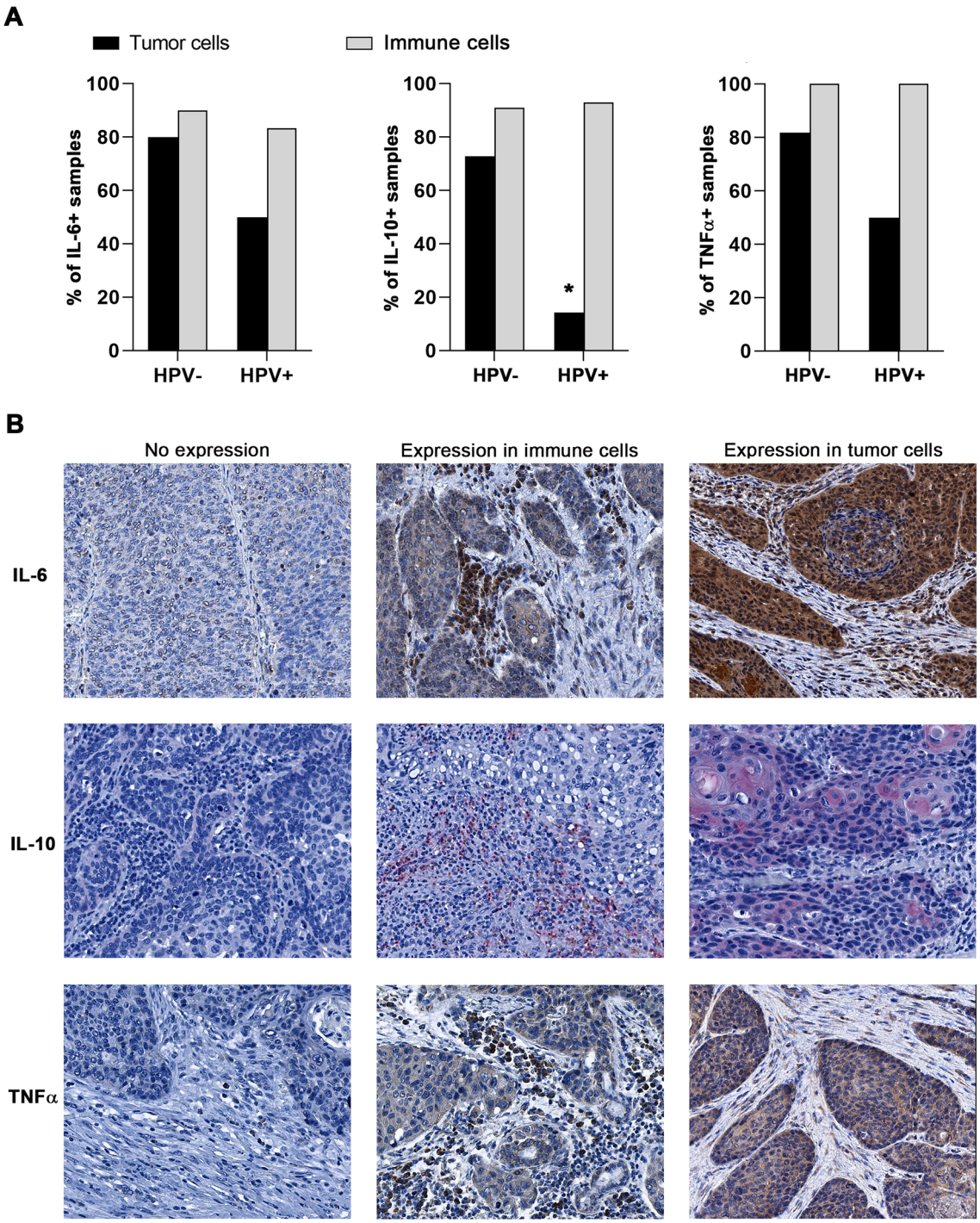

Fig. 4 Production of IL-6, IL-10 and TNFα in tumor cells and tumor-infiltrating immune cells with respect to HPV status. **a** Columns represent the proportions of HPV^+ (n = 14) and HPV^- ($n = 11$) tumor samples expressing IL-6, IL-10 and TNFα in tumor cells (black column) and tumor-infiltrating immune cells (gray column). **b** Representative IHC staining of IL-6, IL-10 and TNFα in tumor-infiltrating immune cells and tumor cells. * $p < 0.05$

agents, namely tobacco/alcohol consumption and HPV infection. HPV-induced tumors are typically located in the oropharynx and are associated with better locoregional control and longer overall survival in response to conventional treatment [3, 4]. Although it has been shown that HPV-associated tumors have a markedly different immune profile than non-virally induced HNSCC [11, 12], so far the functional capacity and phenotype of

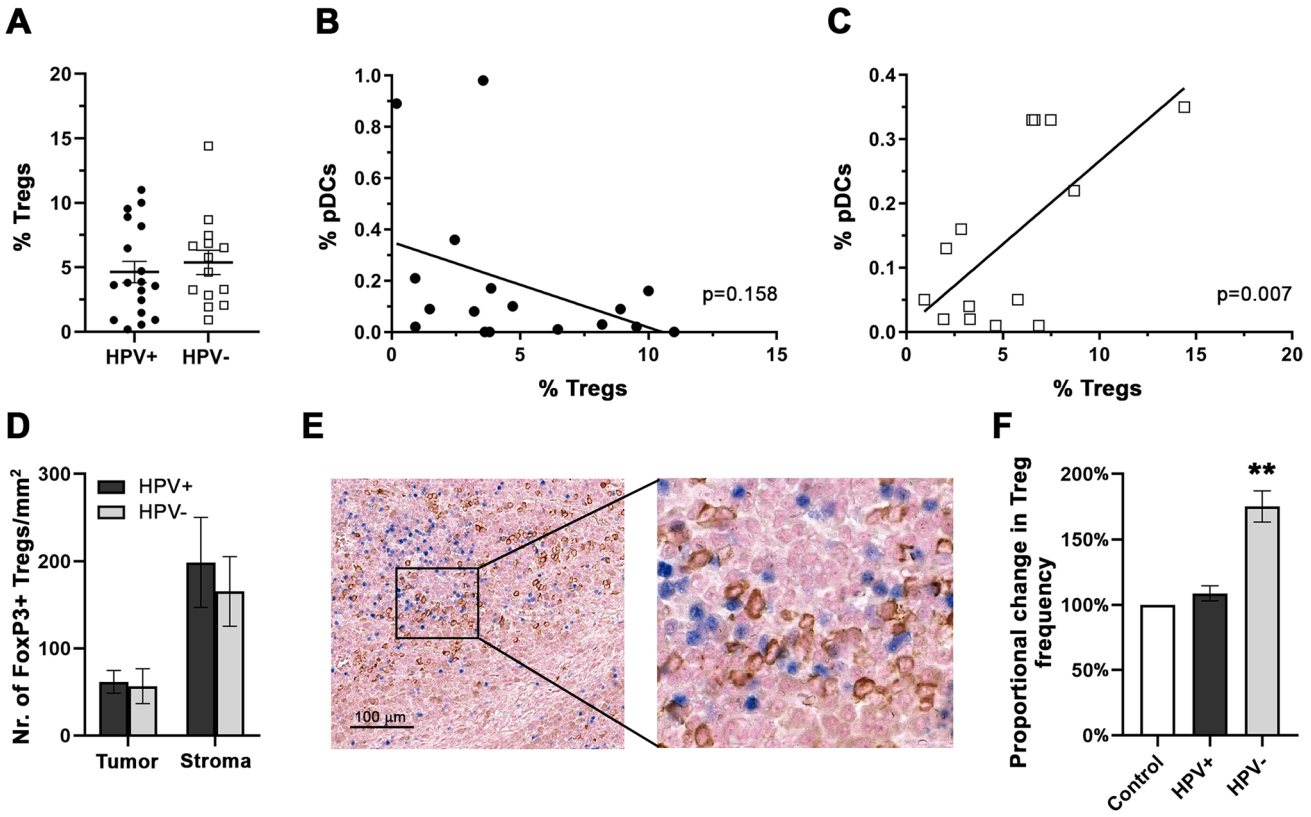

Fig. 5 **a** Frequency of $CD127^{lo}CD25^{hi}FoxP3^{+}CD4^{+}$ Tregs in HPV^{+} ($n=18$) and HPV^{-} ($n=14$) HNSCC patients using flow cytometry analysis. Each symbol represents a patient, the horizontal line represents the average, and error bars indicate SEM. Cells are gated on $CD4^{+}$ tumor-infiltrating T lymphocytes. **b**, **c** Correlation between Treg and pDC proportions in HPV^{+} (b) and HPV^{-} (c) HNSCC patients. Linear trendlines and p values are shown. **d** Columns represent the mean (±SEM) densities of $FoxP3^{+}$ cells in tumor nests and tumor stroma of immunohistochemically stained FFPE sections of HPV^{+} ($n=12$) and HPV^{-} ($n=11$) HNSCC. **e** Colocalization of $FoxP3^{+}$ Tregs (blue nuclei) and BDCA-2^{+} pDCs (brown membranes) in the stroma of a representative HNSCC patient. **f** Columns represent the average change in proportions of Tregs in pDC – CD4 + T cell co-cultures upon cultivating pDCs, derived from peripheral blood of healthy donors, with/without HPV^{+} ($n=7$; black column) and HPV^{-} ($n=7$; gray column) HNSCC cell culture supernatants. Error bars represent SEM. ** $p<0.01$

tumor-infiltrating pDCs have never been evaluated with respect to the HPV status of the tumor.

In the present study, we analyzed the capacity of pDCs to produce IFNα upon stimulation with CpG and imiquimod, in 44 HPV-negative and 32 HPV-positive HNSCC tumor samples. While the densities of pDCs within the tumor microenvironment were comparable in both groups, pDCs derived from HPV-negative samples produced significantly lower amounts of IFNα upon CpG stimulation compared to pDCs derived from HPV-positive tumor tissues and control tonsils. These results correlated with the markedly different cytokine profiles of HPV^{+} vs. HPV^{-} tumors, suggesting that the impaired functional capacity of pDCs infiltrating non-virally induced HNSCC may be caused by a suppressive cytokine milieu in the HPV^{-} tumor microenvironment. In contrast, pDCs derived from HPV^{+} tumors were in most cases functionally unimpaired, with a markedly lower capacity of IFNα production observed in patients who succumbed to the disease during follow-up.

In most of the published studies, the functional capacity of tumor-infiltrating pDCs was compared to the circulating pDCs of the patients. We observed that the functional capacity of blood-derived pDCs markedly decreased with the time of sample processing; therefore, we used healthy tonsils and peritumoral mucosa as control samples, which were processed exactly like the tumor tissue, to avoid any effect of sample processing on pDC functions. We found similar densities of pDCs in all of the tissues analyzed, with slightly higher numbers of pDCs in tonsils, which was in accordance with previously published data [24]. The proportion of IFNα-producing pDCs did not differ between HPV^{+} and HPV^{-} samples; however, the MFI of $IFN\alpha^{+}$ pDCs was significantly higher in CpG-stimulated HPV^{+} tissues compared to HPV^{-} samples. These data suggested that IFNα is produced by similar proportions of pDCs in both HPV^{+}

and HPV$^-$ tumors, but the amounts of secreted IFNα could differ markedly. Therefore, we analyzed the levels of IFNα in culture supernatants harvested from CpG- and IMQ-stimulated tumor-derived single-cell suspensions. In accordance with the flow cytometry data, we observed significantly lower levels of IFNα in supernatants from CpG-stimulated HPV$^-$ tumor suspensions compared to HPV$^+$ tumor suspensions and control tonsils. Upon IMQ stimulation, the production of IFNα was very low, most likely due to a substantial decrease in pDC viability in IMQ-treated cultures, as shown in Fig. S1B.

Fuchs et al. [29] reported that cross-linking of NKp44 expressed on a subset of tonsillar pDCs markedly inhibited the production of IFNα in response to CpG stimulation. To assess whether NKp44 expression may be a hallmark of pDC dysfunction, we analyzed the expression levels of NKp44 in IFNα-producing and IFNα-negative pDCs. Surprisingly, we observed significantly higher expression of NKp44 in HPV$^+$ tumor-derived pDCs compared to pDCs infiltrating HPV$^-$ tumors, with no relationship to IFNα production upon stimulation. In tonsils, NKp44 expression was associated with the production of IL-3 by adjacent memory CD8$^+$ T cells [29]; thus, a higher proportion of NKp44$^+$ pDCs in HPV$^+$ tumors might reflect higher densities of CD8$^+$ T cells within the microenvironment of HPV$^+$ HNSCC [11, 13]. Hartmann et al. [24] observed downregulation of TLR mRNA expression in pDCs incubated in the presence of HNSCC culture supernatants. In our study, we did not observe any differences in the expression of TLR7 and TLR9 at the protein level in pDCs infiltrating HPV$^-$ and HPV$^+$ tumor tissues, nor did we show any significant differences in the expression of other pDC-associated molecules, namely CD28, Granzyme B, IDO, TIM-3 and TRAIL.

Previous studies described the impact of tumor-derived cell culture supernatants on the functional capacity of pDCs infiltrating HNSCC, ovarian, breast and cervical tumors [24, 28, 30–32]. In our study, only HPV$^-$ supernatants significantly inhibited IFNα production in control pDCs, which is in accordance with the observed impairment of functional capacity of pDCs infiltrating HPV$^-$ but not HPV$^+$ tumors. In ovarian and breast cancers, TNFα and TGFβ were shown to be the key factors inducing the impairment of IFNα production [27, 28, 30]. In cervical cancer, the major role was attributed to HMGB1 secreted by neoplastic keratinocytes from the genital tract [32]. Additionally, IL-10 was shown to be a potent inhibitor of both IFNα and IL-12 production of CpG-stimulated pDCs [33]. The design of our experiments enabled us to detect the most pronounced differences in the cytokine milieu between the highly suppressive HPV$^-$ supernatants (suppression of IFNα production $>50\%$) and non-suppressive HPV$^+$ supernatants (suppression $\leq 20\%$). Indeed, we showed that suppressive HPV$^-$ supernatants contained significantly higher levels of IL-6, IL-10 and TNFα but not HMGB1 compared to non-suppressive HPV$^+$ supernatants. In comparison with the concentrations that we observed in the culture supernatants of HNSCC cell suspensions (5.7–49.7 ng/ml), in vitro studies describing the inhibitory effect of HMGB1 on pDC functions [32, 34] used substantially higher concentrations (1–2 µg/ml) of recombinant protein to achieve $>50\%$ inhibition of IFNα production. The relatively low concentrations of HMGB1 in HNSCC suggest that this is most likely not the key factor in pDC inhibition induced by HPV$^-$ tumor environment. In our study, IL-10 and TNFα at the concentrations observed in culture supernatants significantly impaired IFNα production by circulating pDCs, suggesting their important role in mediating pDC dysfunction in HPV$^-$ HNSCC. Indeed, neutralization of TNFα in inhibitory cell culture supernatants restored IFNα production by pDCs to $82.8 \pm 13.5\%$. Considering the fact that neutralization of IL-10 restored IFNα production only to $47.3 \pm 19.9\%$ and no additive effect of neutralization of multiple cytokines was observed, TNFα seems to be the key factor in HPV$^-$ HNSCC microenvironment, which suppresses tumor-infiltrating pDCs.

In HNSCC, TNFα was shown to be mainly produced by tumor cells and macrophages [35, 36]. Indeed, our data revealed TNFα-positive staining of tumor cells in 81.8% of HPV$^-$ samples compared to 50% of HPV$^+$ samples. Similarly, IL-10-positive tumor cells were detected in 72.7% of HPV$^-$ tissues, but only in 14.3% of HPV$^+$ tissues.

It has been reported that functionally impaired pDCs promote selective Treg expansion and are capable of priming Tregs by the ICOS/ICOS-L pathway [20, 37, 38]. Consistent with these data, we observed a significant positive correlation between Treg and pDC proportions in HPV$^-$ but not HPV$^+$ HNSCC. Additionally, FoxP3$^+$ Tregs colocalized with BDCA-2$^+$ pDCs in the tumor stroma of HPV$^-$ tumor samples, suggesting interactions between pDCs and Tregs in the HNSCC tumor microenvironment. Indeed, we showed that pDCs from healthy donors affected by HPV$^-$ but not by HPV$^+$ HNSCC cell culture supernatants are capable to induce Treg expansion. Thus, we suggest that the environment of HPV$^-$ HNSCC is capable to drive pDCs to become potent inducers of Treg expansion, promoting immunosuppression in the tumor. Tumor-infiltrating Tregs were reported to be major drivers of resistance to radiotherapy and PD-L1 blockade in HNSCC mouse model [39]. In HPV$^-$ HNSCC, tumor-infiltrating pDCs, which support Treg expansion, thus might represent an underestimated target for future immunotherapeutic approaches. However, the exact contribution of pDC-induced Treg expansion to the total levels of tumor-infiltrating Tregs needs further evaluation in vivo.

In conclusion, our study shows that the highly immunosuppressive cytokine milieu in HPV$^-$ but not in HPV$^+$ HNSCC significantly affects the functional capacity of

tumor-infiltrating pDCs. Such dysfunctional pDCs most likely further support the suppressive microenvironment by promoting the expansion of Tregs in the tumor tissue. Targeting pDCs in HPV$^-$ HNSCC thus might represent a promising therapeutic strategy that could disrupt the vicious cycle intensifying the immunosuppressive setting of the tumor microenvironment.

Supplementary Information The online version contains supplementary material available at (https://doi.org/10.1007/s00262-021-02874-y).

Acknowledgements The major sponsor of this study was Sotio a.s. The project was partly supported by the Grant Agency of Charles University in Prague, project No. 668217. We thank the nursing and medical staff at the Department of Otorhinolaryngology and Head and Neck Surgery, First Medical Faculty, Motol University Hospital, for their indispensable cooperation in the study.

Author contributions VK designed and performed the experiments, collected native tumor tissue and blood samples, collected and evaluated clinical data and wrote the article; KH and ET performed the experiments and provided critical reading of the manuscript; JB coordinated collection of the native tumor tissue samples and clinical data and provided critical reading of the manuscript; MG prepared paraffin-embedded sections and native tumor tissue samples and provided pathologic staging of the patients; RS supervised design of the study and performed critical reading of the manuscript; AF designed the study, supervised experiments, performed data analysis and wrote the article.

Funding The major sponsor of this study was Sotio a.s. The project was partly supported by the Grant Agency of Charles University in Prague, project No. 668217.

Data availability and material Data are available on a reasonable request from the corresponding authors.

Compliance with ethical standards

Conflict of interest Vladimír Koucký, Kamila Hladíková, Eliška Táborská, Radek Špíšek and Anna Fialová are employees of Sotio, a biotechnological company, which develops new therapies focusing on the treatment of cancer and autoimmune diseases. Authors declare no competing financial interests.

Consent to participate All patients and healthy donors enrolled in this study signed an informed consent, which was approved by the Ethics Committee of the Motol University Hospital, Prague, Czech Republic.

Ethics approval All procedures performed in this study were in accordance with the ethical standards of the institutional and national research committee and with the 1964 Declaration of Helsinki and its later amendments. The study was approved by the Ethics Committee of the Motol University Hospital, Prague, Czech Republic (No. 1320/16).

References

1. Mork J, Lie AK, Glattre E, Hallmans G, Jellum E, Koskela P, Moller B, Pukkala E, Schiller JT, Youngman L, Lehtinen M, Dillner J (2001) Human papillomavirus infection as a risk factor for squamous-cell carcinoma of the head and neck. N Engl J Med 344(15):1125–1131. https://doi.org/10.1056/NEJM200104123441503
2. Kreimer AR, Clifford GM, Boyle P, Franceschi S (2005) Human papillomavirus types in head and neck squamous cell carcinomas worldwide: a systematic review. Cancer Epidemiol Biomarkers Prev 14(2):467–475. https://doi.org/10.1158/1055-9965.EPI-04-0551
3. Ang KK, Harris J, Wheeler R, Weber R, Rosenthal DI, Nguyen-Tan PF, Westra WH, Chung CH, Jordan RC, Lu C, Kim H, Axelrod R, Silverman CC, Redmond KP, Gillison ML (2010) Human papillomavirus and survival of patients with oropharyngeal cancer. N Engl J Med 363(1):24–35. https://doi.org/10.1056/NEJMoa0912217
4. Fakhry C, Westra WH, Li S, Cmelak A, Ridge JA, Pinto H, Forastiere A, Gillison ML (2008) Improved survival of patients with human papillomavirus-positive head and neck squamous cell carcinoma in a prospective clinical trial. J Natl Cancer Inst 100(4):261–269. https://doi.org/10.1093/jnci/djn011
5. El-Naggar AK, Westra WH (2012) p16 expression as a surrogate marker for HPV-related oropharyngeal carcinoma: a guide for interpretative relevance and consistency. Head Neck 34(4):459–461. https://doi.org/10.1002/hed.21974
6. Lydiatt WM, Patel SG, O'Sullivan B, Brandwein MS, Ridge JA, Migliacci JC, Loomis AM, Shah JP (2017) Head and Neck cancers-major changes in the American Joint Committee on cancer eighth edition cancer staging manual. CA Cancer J Clin 67 (2):122–137. doi:https://doi.org/10.3322/caac.21389
7. Network NCC NCCN Clinical Practice Guidelines in Oncology, Head and Neck Cancers (Version 1/2018). https://www.nccn.org/.
8. Deschuymer S, Mehanna H, Nuyts S (2018) Toxicity Reduction in the Treatment of HPV Positive Oropharyngeal Cancer: Emerging Combined Modality Approaches. Front Oncol 8:439. https://doi.org/10.3389/fonc.2018.00439
9. Ferris RL, Blumenschein G Jr, Fayette J, Guigay J, Colevas AD, Licitra L, Harrington K, Kasper S, Vokes EE, Even C, Worden F, Saba NF, Iglesias Docampo LC, Haddad R, Rordorf T, Kiyota N, Tahara M, Monga M, Lynch M, Geese WJ, Kopit J, Shaw JW, Gillison ML (2016) Nivolumab for recurrent squamous-cell carcinoma of the head and neck. N Engl J Med 375(19):1856–1867. https://doi.org/10.1056/NEJMoa1602252
10. Mehra R, Seiwert TY, Gupta S, Weiss J, Gluck I, Eder JP, Burtness B, Tahara M, Keam B, Kang H, Muro K, Geva R, Chung HC, Lin CC, Aurora-Garg D, Ray A, Pathiraja K, Cheng J, Chow LQM, Haddad R (2018) Efficacy and safety of pembrolizumab in recurrent/metastatic head and neck squamous cell carcinoma: pooled analyses after long-term follow-up in KEYNOTE-012. Br J Cancer 119(2):153–159. https://doi.org/10.1038/s41416-018-0131-9
11. Partlova S, Boucek J, Kloudova K, Lukesova E, Zabrodsky M, Grega M, Fucikova J, Truxova I, Tachezy R, Spisek R, Fialova A (2015) Distinct patterns of intratumoral immune cell infiltrates in patients with HPV-associated compared to non-virally induced head and neck squamous cell carcinoma. Oncoimmunology 4(1):e965570. https://doi.org/10.4161/21624011.2014.965570
12. Mandal R, Senbabaoglu Y, Desrichard A, Havel JJ, Dalin MG, Riaz N, Lee KW, Ganly I, Hakimi AA, Chan TA, Morris LG (2016) The head and neck cancer immune landscape and its immunotherapeutic implications. JCI Insight 1(17):e89829. https://doi.org/10.1172/jci.insight.89829
13. Hladikova K, Koucky V, Boucek J, Laco J, Grega M, Hodek M, Zabrodsky M, Vosmik M, Rozkosova K, Vosmikova H, Celakovsky P, Chrobok V, Ryska A, Spisek R, Fialova A (2019) Tumor-infiltrating B cells affect the progression of oropharyngeal squamous cell carcinoma via cell-to-cell interactions with CD8(+)

T cells. J Immunother Cancer 7(1):261. https://doi.org/10.1186/s40425-019-0726-6
14. Dzionek A, Sohma Y, Nagafune J, Cella M, Colonna M, Facchetti F, Gunther G, Johnston I, Lanzavecchia A, Nagasaka T, Okada T, Vermi W, Winkels G, Yamamoto T, Zysk M, Yamaguchi Y, Schmitz J (2001) BDCA-2, a novel plasmacytoid dendritic cell-specific type II C-type lectin, mediates antigen capture and is a potent inhibitor of interferon alpha/beta induction. J Exp Med 194(12):1823–1834
15. Dzionek A, Fuchs A, Schmidt P, Cremer S, Zysk M, Miltenyi S, Buck DW, Schmitz J (2000) BDCA-2, BDCA-3, and BDCA-4: three markers for distinct subsets of dendritic cells in human peripheral blood. J Immunol 165(11):6037–6046
16. Tel J, Smits EL, Anguille S, Joshi RN, Figdor CG, de Vries IJ (2012) Human plasmacytoid dendritic cells are equipped with antigen-presenting and tumoricidal capacities. Blood 120(19):3936–3944. https://doi.org/10.1182/blood-2012-06-435941
17. Martin-Gayo E, Sierra-Filardi E, Corbi AL, Toribio ML (2010) Plasmacytoid dendritic cells resident in human thymus drive natural Treg cell development. Blood 115(26):5366–5375. https://doi.org/10.1182/blood-2009-10-248260
18. Chaperot L, Blum A, Manches O, Lui G, Angel J, Molens JP, Plumas J (2006) Virus or TLR agonists induce TRAIL-mediated cytotoxic activity of plasmacytoid dendritic cells. J Immunol 176(1):248–255
19. Liu C, Lou Y, Lizee G, Qin H, Liu S, Rabinovich B, Kim GJ, Wang YH, Ye Y, Sikora AG, Overwijk WW, Liu YJ, Wang G, Hwu P (2008) Plasmacytoid dendritic cells induce NK cell-dependent, tumor antigen-specific T cell cross-priming and tumor regression in mice. J Clin Invest 118(3):1165–1175. https://doi.org/10.1172/JCI33583
20. Koucky V, Boucek J, Fialova A (2019) Immunology of plasmacytoid dendritic cells in solid tumors: a brief review. Cancers. https://doi.org/10.3390/cancers11040470
21. Treilleux I, Blay JY, Bendriss-Vermare N, Ray-Coquard I, Bachelot T, Guastalla JP, Bremond A, Goddard S, Pin JJ, Barthelemy-Dubois C, Lebecque S (2004) Dendritic cell infiltration and prognosis of early stage breast cancer. Clin Cancer Res 10(22):7466–7474. https://doi.org/10.1158/1078-0432.CCR-04-0684
22. Labidi-Galy SI, Treilleux I, Goddard-Leon S, Combes JD, Blay JY, Ray-Coquard I, Caux C, Bendriss-Vermare N (2012) Plasmacytoid dendritic cells infiltrating ovarian cancer are associated with poor prognosis. Oncoimmunology 1(3):380–382. https://doi.org/10.4161/onci.18801
23. Jensen TO, Schmidt H, Moller HJ, Donskov F, Hoyer M, Sjoegren P, Christensen IJ, Steiniche T (2012) Intratumoral neutrophils and plasmacytoid dendritic cells indicate poor prognosis and are associated with pSTAT3 expression in AJCC stage I/II melanoma. Cancer 118(9):2476–2485. https://doi.org/10.1002/cncr.26511
24. Hartmann E, Wollenberg B, Rothenfusser S, Wagner M, Wellisch D, Mack B, Giese T, Gires O, Endres S, Hartmann G (2003) Identification and functional analysis of tumor-infiltrating plasmacytoid dendritic cells in head and neck cancer. Cancer Res 63(19):6478–6487
25. Han N, Zhang Z, Liu S, Ow A, Ruan M, Yang W, Zhang C (2017) Increased tumor-infiltrating plasmacytoid dendritic cells predicts poor prognosis in oral squamous cell carcinoma. Arch Oral Biol 78:129–134. https://doi.org/10.1016/j.archoralbio.2017.02.012
26. Yang LL, Mao L, Wu H, Chen L, Deng WW, Xiao Y, Li H, Zhang L, Sun ZJ (2019) pDC depletion induced by CD317 blockade drives the antitumor immune response in head and neck squamous cell carcinoma. Oral Oncol 96:131–139. https://doi.org/10.1016/j.oraloncology.2019.07.019
27. Sisirak V, Faget J, Vey N, Blay JY, Menetrier-Caux C, Caux C, Bendriss-Vermare N (2013) Plasmacytoid dendritic cells deficient in IFNalpha production promote the amplification of FOXP3(+) regulatory T cells and are associated with poor prognosis in breast cancer patients. Oncoimmunology 2(1):e22338. https://doi.org/10.4161/onci.22338
28. Sisirak V, Vey N, Goutagny N, Renaudineau S, Malfroy M, Thys S, Treilleux I, Labidi-Galy SI, Bachelot T, Dezutter-Dambuyant C, Menetrier-Caux C, Blay JY, Caux C, Bendriss-Vermare N (2013) Breast cancer-derived transforming growth factor-beta and tumor necrosis factor-alpha compromise interferon-alpha production by tumor-associated plasmacytoid dendritic cells. Int J Cancer 133(3):771–778. https://doi.org/10.1002/ijc.28072
29. Fuchs A, Cella M, Kondo T, Colonna M (2005) Paradoxic inhibition of human natural interferon-producing cells by the activating receptor NKp44. Blood 106(6):2076–2082. https://doi.org/10.1182/blood-2004-12-4802
30. Labidi-Galy SI, Sisirak V, Meeus P, Gobert M, Treilleux I, Bajard A, Combes JD, Faget J, Mithieux F, Cassignol A, Tredan O, Durand I, Menetrier-Caux C, Caux C, Blay JY, Ray-Coquard I, Bendriss-Vermare N (2011) Quantitative and functional alterations of plasmacytoid dendritic cells contribute to immune tolerance in ovarian cancer. Cancer Res 71(16):5423–5434. https://doi.org/10.1158/0008-5472.CAN-11-0367
31. Bruchhage KL, Heinrichs S, Wollenberg B, Pries R (2018) IL-10 in the microenvironment of HNSCC inhibits the CpG ODN induced IFN-alpha secretion of pDCs. Oncol Lett 15(3):3985–3990. https://doi.org/10.3892/ol.2018.7772
32. Demoulin S, Herfs M, Somja J, Roncarati P, Delvenne P, Hubert P (2015) HMGB1 secretion during cervical carcinogenesis promotes the acquisition of a tolerogenic functionality by plasmacytoid dendritic cells. Int J Cancer 137(2):345–358. https://doi.org/10.1002/ijc.29389
33. Duramad O, Fearon KL, Chan JH, Kanzler H, Marshall JD, Coffman RL, Barrat FJ (2003) IL-10 regulates plasmacytoid dendritic cell response to CpG-containing immunostimulatory sequences. Blood 102(13):4487–4492. https://doi.org/10.1182/blood-2003-07-2465
34. Popovic PJ, DeMarco R, Lotze MT, Winikoff SE, Bartlett DL, Krieg AM, Guo ZS, Brown CK, Tracey KJ, Zeh HJ 3rd (2006) High mobility group B1 protein suppresses the human plasmacytoid dendritic cell response to TLR9 agonists. J Immunol 177(12):8701–8707. https://doi.org/10.4049/jimmunol.177.12.8701
35. Parks RR, Yan SD, Huang CC (1994) Tumor necrosis factor-alpha production in human head and neck squamous cell carcinoma. Laryngoscope 104(7):860–864. https://doi.org/10.1288/00005537-199407000-00015
36. Nakano Y, Kobayashi W, Sugai S, Kimura H, Yagihashi S (1999) Expression of tumor necrosis factor-alpha and interleukin-6 in oral squamous cell carcinoma. Jpn J Cancer Res 90(8):858–866. https://doi.org/10.1111/j.1349-7006.1999.tb00827.x
37. Ito T, Yang M, Wang YH, Lande R, Gregorio J, Perng OA, Qin XF, Liu YJ, Gilliet M (2007) Plasmacytoid dendritic cells prime IL-10-producing T regulatory cells by inducible costimulator ligand. J Exp Med 204(1):105–115. https://doi.org/10.1084/jem.20061660
38. Sisirak V, Faget J, Gobert M, Goutagny N, Vey N, Treilleux I, Renaudineau S, Poyet G, Labidi-Galy SI, Goddard-Leon S, Durand I, Le Mercier I, Bajard A, Bachelot T, Puisieux A, Puisieux I, Blay JY, Menetrier-Caux C, Caux C, Bendriss-Vermare N (2012) Impaired IFN-alpha production by plasmacytoid dendritic cells favors regulatory T-cell expansion that may contribute to breast cancer progression. Cancer Res 72(20):5188–5197. https://doi.org/10.1158/0008-5472.CAN-11-3468

39. Oweida A, Hararah MK, Phan A, Binder D, Bhatia S, Lennon S, Bukkapatnam S, Van Court B, Uyanga N, Darragh L, Kim HM, Raben D, Tan AC, Heasley L, Clambey E, Nemenoff R, Karam SD (2018) Resistance to radiotherapy and PD-L1 blockade is mediated by TIM-3 upregulation and regulatory T-Cell infiltration. Clin Cancer Res 24(21):5368–5380. https://doi.org/10.1158/1078-0432.CCR-18-1038